

Sains Malaysiana 43(3)(2014): 437–441

## Synthesis and Photocatalysis of ZnO/ $\gamma$ -Fe<sub>2</sub>O<sub>3</sub> Nanocomposite in Degrading Herbicide 2,4-dichlorophenoxyacetic Acid

(Sintesis dan Fotokatalisis ZnO/ $\gamma$ -Fe<sub>2</sub>O<sub>3</sub> dalam Mendegradasi Herbisid Asid 2,4-diklorofenoksiasetik)

LEE KIAN MUN, ABDUL HALIM ABDULLAH\*, MOHD ZOBIR HUSSEIN & ZULKARNAIN ZAINAL

### ABSTRACT

ZnO/ $\gamma$ -Fe<sub>2</sub>O<sub>3</sub> catalysts were fabricated via a simple precipitation route using zinc acetate and iron acetate as the precursors and ammonia as the precipitant. The resulted nanocatalysts were subjected to heat treatment at 450°C for 2 h. The characteristics of the nanocomposite were investigated by various characterization techniques. The synthesized nanocomposite has an average particle size of 13 nm and a surface area of 17 m<sup>2</sup>/g. The photocatalytic activity of ZnO/ $\gamma$ -Fe<sub>2</sub>O<sub>3</sub> nanocomposite was evaluated by photodegrading 2,4-dichlorophenoxyacetic acid (2,4-D) under UV irradiation. The results showed that ZnO/ $\gamma$ -Fe<sub>2</sub>O<sub>3</sub> nanocomposite exhibited enhanced photoactivity compared to pure ZnO with almost 20% increment within 4 h of reaction time. The result indicated the applicability of ZnO/ $\gamma$ -Fe<sub>2</sub>O<sub>3</sub> nanocomposite to be used as photocatalyst in removing organic pollutants in wastewater.

**Keywords:** Photocatalytic degradation; precipitation; zinc oxide; 2,4-D

### ABSTRAK

Mangkin ZnO/ $\gamma$ -Fe<sub>2</sub>O<sub>3</sub> telah disintesis dengan kaedah pemendakan dengan menggunakan zink asetat dihidrat dan ferum asetat sebagai bahan pemula dan ammonia sebagai agen pemendak. Nanomangkin yang dihasilkan dikalsin pada 450°C selama 2 jam. Ciri mangkin yang dihasilkan dikaji dengan pelbagai analisis. ZnO/ $\gamma$ -Fe<sub>2</sub>O<sub>3</sub> yang dihasilkan mempunyai purata saiz zarah sebesar 13 nm dan luas permukaan sebanyak 17 m<sup>2</sup>/g. Aktiviti fotopemangkinan bagi ZnO/ $\gamma$ -Fe<sub>2</sub>O<sub>3</sub> yang disintesis telah dinilai dengan mendegradasi asid 2,4-diklorofenoksiasetik (2,4-D) di bawah radiasi cahaya ultraungu. Kajian menunjukkan bahawa peratusan penyingkiran 2,4-D oleh ZnO/ $\gamma$ -Fe<sub>2</sub>O<sub>3</sub> melebihi ZnO sebanyak 20% dalam masa 4 jam. Ini menunjukkan ZnO/ $\gamma$ -Fe<sub>2</sub>O<sub>3</sub> yang dihasilkan mampu diaplikasikan sebagai fotomangkin untuk menyingkirkan pencemar organik dalam air sisa.

**Kata kunci:** Fotokatalisis degradasi; pemendakan; zink oksida; 2,4-D

### INTRODUCTION

Heterogeneous photocatalysis has drawn major attention due to its capability in removing various types of organic contaminants (Gaya et al. 2010; Rao et al. 2009; Sobana & Swaminathan 2007; Uddin et al. 2007; Xie et al. 2011). This ultimate process is based on the generation of highly reactive hydroxyl radicals to mineralize organic carbon into carbon dioxide and water (Konstantinou & Albanis 2004; Pera-Titus et al. 2004). The application of titania (TiO<sub>2</sub>) in photocatalysis has been studied intensively due to its excellent photocatalytic activity (Baran et al. 2008; Pourata et al. 2009; Saïen & Khezrianjoo 2008). The ability of TiO<sub>2</sub> working in a wide range of pH and chemically stable make it superior in wastewater treatment. Zinc oxide (ZnO) has received considerable interest as a suitable alternative photocatalyst to titania due to its similar band gap energy (3.2 eV) (Akyol & Bayramoglu 2005; Daneshvar et al. 2004; Evgenidou et al. 2005). In some cases, ZnO even showed better photodegradation efficiency compared to titania (Khodja et al. 2001 & Lizama et al. 2002).

One of the major drawbacks in heterogeneous photocatalysis is the recombination of photogenerated hole (h<sup>+</sup>) and electron (e<sup>-</sup>). This recombination step lowers the quantum yield and cause energy wasting. Therefore, the e<sup>-</sup>-h<sup>+</sup> recombination process should be inhibited to ensure efficient photocatalysis. Coupled semiconductor has been proven to enhance the charge separation of electron-hole pair which increase the lifetime of the charge carriers and consequently reduce the recombination of electron-hole. As a result, higher degradation rate was observed (Li et al. 2011; Lin et al. 2008; Liu et al. 2008; Nayak et al. 2008; Vaezi 2008).

To our best knowledge, there are only a few reports in synthesizing ZnO/ $\gamma$ -Fe<sub>2</sub>O<sub>3</sub> nanocomposite structure (Fu et al. 2008; Wu et al. 2010). Moreover, the utilization of ZnO/ $\gamma$ -Fe<sub>2</sub>O<sub>3</sub> in degrading 2,4-dichlorophenoxyacetic acid (2,4-D) has not been reported so far. In this paper, ZnO/ $\gamma$ -Fe<sub>2</sub>O<sub>3</sub> nanocomposite was obtained via precipitation method. The characteristics of the resulting catalyst and its efficiency in the degradation of 2,4-D were also examined.

## MATERIALS AND METHODS

All the chemicals and reagents used in this study, i.e. zinc acetate dihydrate ( $\text{Zn}(\text{CH}_3\text{COO})_2 \cdot 2\text{H}_2\text{O}$ , Merck), ammonia solution (25% v/v,  $\text{NH}_3 \cdot \text{H}_2\text{O}$ , Merck), iron acetate ( $\text{Fe}(\text{CH}_3\text{COO})_2$ , Aldrich) and 2,4-dichlorophenoxyacetic acid (2,4-D, Fluka) are A.R. grade and were used without any purification. Deionized water was used throughout the studies.

0.01 mole of  $\text{Zn}(\text{CH}_3\text{COO})_2 \cdot 2\text{H}_2\text{O}$  and 0.001 mole of  $\text{Fe}(\text{CH}_3\text{COO})_2$  were dissolved in 100 mL deionized water at room temperature under vigorous stirring. Then, ammonia solution was added drop wise into the above solution with stirring. The precipitates formed were centrifuged, washed with deionized water and finally oven-dried at  $110^\circ\text{C}$  overnight. The procedure was repeated in preparing pure ZnO excluded the addition of iron acetate. The resulted powder (ZnO and ZnO/ $\gamma\text{-Fe}_2\text{O}_3$  composite) was calcined at  $450^\circ\text{C}$  for 2 h.

The obtained products were characterized by XRD (Shimadzu XRD-6000 Diffractometer), TEM (Hitachi 7100), EDX (JEOL JSM 6400) and BET surface area (Autosorb AS-1, Quantachrome). Free software ImageJ was used to measure the particle size of the catalyst on TEM micrograph while SPSS software (IBM) was applied in constructing the particle size distribution histogram.

The photodegradation efficiency of the synthesized pure ZnO and ZnO/ $\gamma\text{-Fe}_2\text{O}_3$  nanocomposite was evaluated by photodegrading (2,4-D) in a photoreactor under 6 W UV-A irradiation (Hitachi). The solution was stirred for 15 min at speed of 280 rpm to attain adsorption equilibrium before irradiation. During irradiation, agitation was maintained by a magnetic stirrer and air was bubbled into the reaction medium to ensure a constant supply of oxygen

( $2 \text{ L min}^{-1}$ ). Test samples were withdrawn at regular time interval and were immediately filtered by using  $0.45 \mu\text{m}$  cellulose nitrate filter to remove catalyst particles. The concentration of 2,4-D in test samples was determined by using Perkin Elmer Lambda 35 UV-Vis spectrophotometer at  $\lambda_{\text{max}} = 283.4 \text{ nm}$ .

## RESULTS AND DISCUSSION

Figure 1(a) and 1(b) depicts the XRD patterns of the synthesized pure ZnO and ZnO/ $\gamma\text{-Fe}_2\text{O}_3$  nanocomposite. Both products exhibited the typical pattern of hexagonal structure of ZnO (JCPDS no.: 36-1451). Peak associated with  $\text{Fe}_2\text{O}_3$  were also observed, which agreed with cubic structure of  $\gamma\text{-Fe}_2\text{O}_3$  (JCPDS card no.: 39-1346). No other impurity peak was detected in XRD pattern of the sample.

The obtained catalysts were further characterized by TEM. As shown in Figure 2, the resulted catalysts have a spherical shape in morphology. The average particle size of the catalysts was determined from the particle size distribution histogram. As observed, the average particle size of pure ZnO and ZnO/ $\gamma\text{-Fe}_2\text{O}_3$  nanocomposite were 31 and 13 nm, respectively.

The surface area of pure ZnO and ZnO/ $\gamma\text{-Fe}_2\text{O}_3$  nanocomposite was measured by BET technique. The results revealed that the pure ZnO and ZnO/ $\gamma\text{-Fe}_2\text{O}_3$  nanocomposite had a surface area of 8 and  $17 \text{ m}^2/\text{g}$ , respectively. This observation was supported by particle size distribution histogram from TEM, where larger particle size resulting in smaller specific surface area.

Figure 3 illustrates photoactivity of pure ZnO and ZnO/ $\gamma\text{-Fe}_2\text{O}_3$  nanocomposite by applying 2,4-D as the modal pollutant. The removal experiments were conducted in triplicate to ensure the reproducibility of the results.

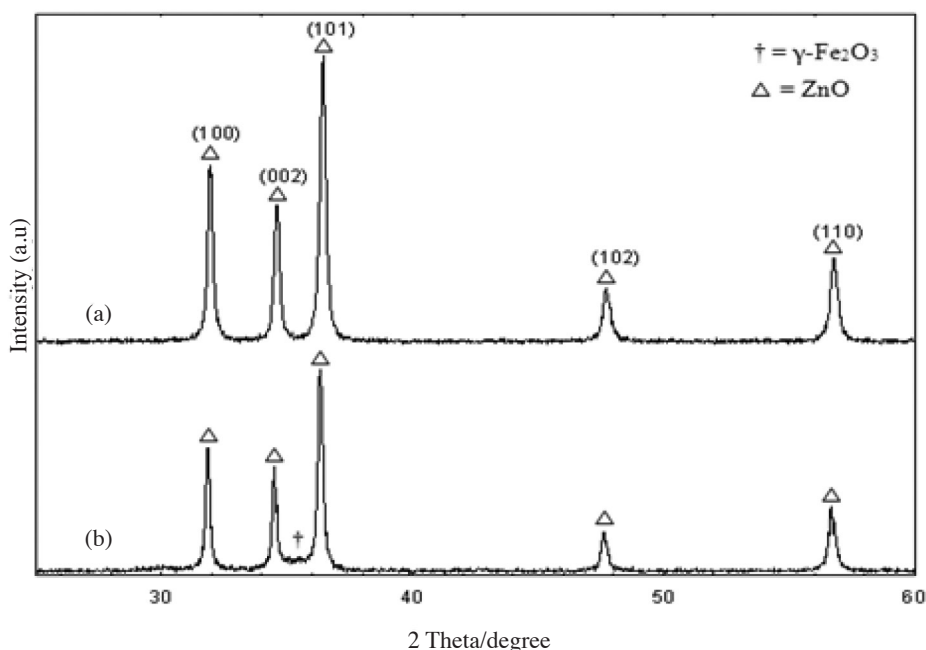


FIGURE 1. XRD patterns of (a) pure ZnO and (b) ZnO/ $\gamma\text{-Fe}_2\text{O}_3$  nanocomposite

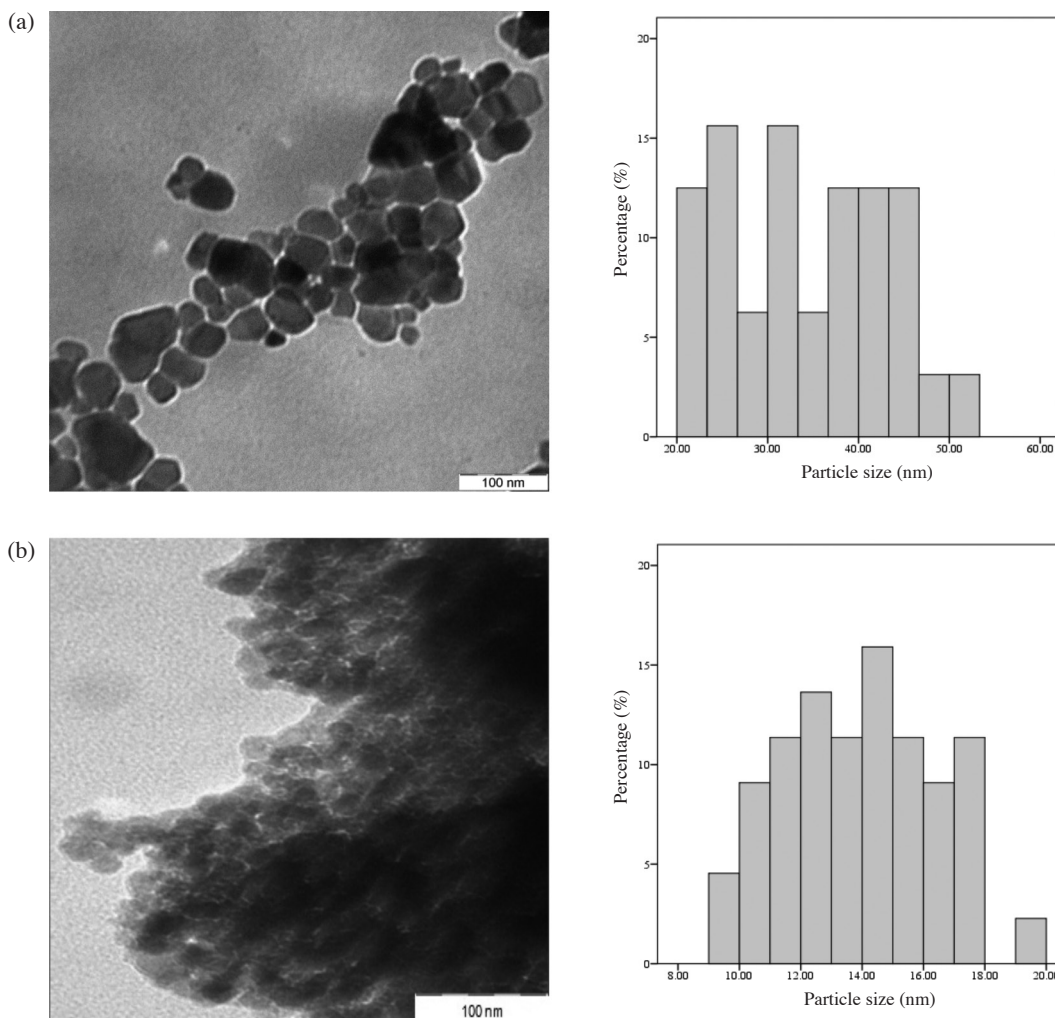


FIGURE 2. TEM image and particle size distribution histogram of (a) pure ZnO and (b) ZnO/ $\gamma$ -Fe<sub>2</sub>O<sub>3</sub> nanocomposite

It can be seen that there is no noticeable change in the concentration of 2,4-D either in photolysis or adsorption test. The results also showed that ZnO/ $\gamma$ -Fe<sub>2</sub>O<sub>3</sub> shows superior photoactivity towards 2,4-D as compared to bare ZnO. This can be explained by larger particles were observed for ZnO compared to ZnO/ $\gamma$ -Fe<sub>2</sub>O<sub>3</sub> from TEM, which caused the loss in surface area. It has been reported that catalyst with higher surface area increased the number of active sites on the catalyst surface, which in turn facilitates the generation of hydroxyl and superoxide radicals (Dodd et al. 2006; Wang et al. 2007). In addition, larger particles increased the recombination rate of electron-hole pairs, due to their slow arrival to reaction sites at the catalyst surface (Jing et al. 2001; Karunakaran & Dhanalakshmi 2008). Another possible explanation is that the conduction band of ZnO and Fe<sub>2</sub>O<sub>3</sub> are very close to each other as shown in Figure 4. Therefore, the injection of electrons from the conduction band of Fe<sub>2</sub>O<sub>3</sub> into ZnO could occur easily, which facilitates its reaction with molecular oxygen to form superoxide radicals. Moreover, the photogenerated holes can then be transferred more efficiently to the surrounding water matrix to produce more

hydroxyl radicals. Consequently, the recombination rate of electron-hole pairs decreased. Thus, the degradation efficiency of 2,4-D was enhanced.

#### CONCLUSION

ZnO and ZnO/ $\gamma$ -Fe<sub>2</sub>O<sub>3</sub> nanocomposite were successfully prepared via precipitation route. TEM analysis showed that nearly spherical morphology was obtained. The average particles size of ZnO and ZnO/ $\gamma$ -Fe<sub>2</sub>O<sub>3</sub> nanocomposite was 13 and 31 nm, respectively. ZnO/ $\gamma$ -Fe<sub>2</sub>O<sub>3</sub> nanocomposite exhibited better photodegradation ability than that of pure ZnO. Therefore, ZnO/ $\gamma$ -Fe<sub>2</sub>O<sub>3</sub> nanocomposite can be potentially applied in removing organic-polluted wastewater.

#### ACKNOWLEDGEMENTS

The authors wish to thank the grant awarded (Research University Grant Scheme, vot.no. 91817). Financial support from Ministry of Science, Technology and Innovation, Malaysia in term of National Science Fellowship (Lee Kian Mun) is also acknowledged.

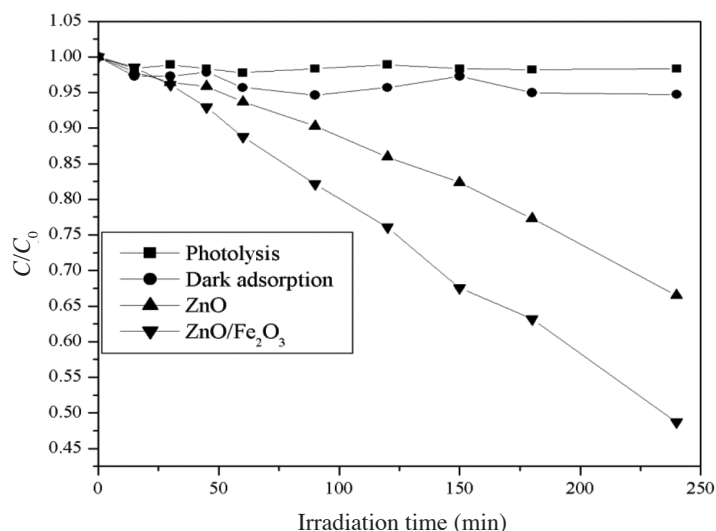


FIGURE 3. Photodegradation of 2,4-D by ZnO and ZnO/ $\gamma$ -Fe<sub>2</sub>O<sub>3</sub> nanocomposite

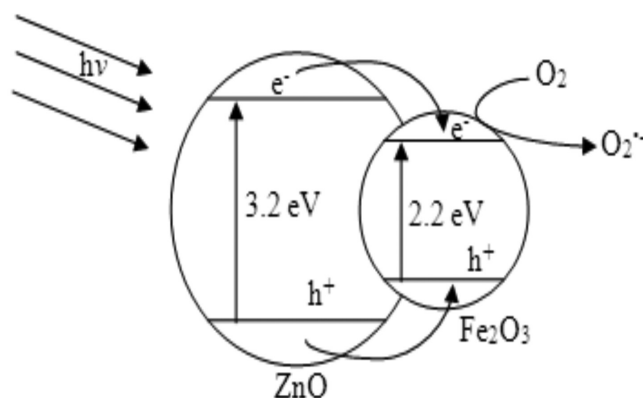


FIGURE 4. Heterojunction of ZnO/ $\gamma$ -Fe<sub>2</sub>O<sub>3</sub> nanocomposite system

#### REFERENCES

- Akyol, A. & Bayramoğlu, M. 2005. Photocatalytic degradation of remazol red F3B using ZnO catalyst. *Journal of Hazardous Materials* 124(1-3): 241-246.
- Baran, W., Adamek, E. & Makowski, A. 2008. The influence of selected parameters on the photocatalytic degradation of azo-dyes in the presence of TiO<sub>2</sub> aqueous suspension. *Chemical Engineering Journal* 145(2): 242-248.
- Daneshvar, N., Salari, D. & Khataee, A.R. 2004. Photocatalytic degradation of azo dye Acid Red 14 in water on ZnO as an alternative catalyst to TiO<sub>2</sub>. *Journal of Photochemistry and Photobiology A: Chemistry* 162(2-3): 317-322.
- Dodd, A.C., McKinley, A.J., Saunders, M. & Tsuzuki, T. 2006. Effect of particle size on the photocatalytic activity of nanoparticulate zinc oxide. *Journal of Nanoparticle Research* 8(1): 43-51.
- Evgenidou, E., Fytianos, K. & Poullos, I. 2005. Semiconductor-sensitized photodegradation of dichlorvos in water using TiO<sub>2</sub> and ZnO as catalysts. *Applied Catalysis B: Environmental* 59(1-2): 81-89.
- Fu, R., Wang, W., Han, R. & Chen, K. 2008. Preparation and characterization of  $\gamma$ -Fe<sub>2</sub>O<sub>3</sub>/ZnO composite particles. *Materials Letters* 62(25): 4066-4068.
- Gaya, U.I., Abdullah, A.H., Hussein, M.Z. & Zainal, Z. 2010. Photocatalytic removal of 2,4,6-trichlorophenol from water exploiting commercial ZnO powder. *Desalination* 263(1-3): 176-182.
- Jing, L., Xu, Z., Sun, X., Jing, S. & Cai, W. 2001. The surface properties and photocatalytic activities of ZnO ultrafine particles. *Applied Surface Science* 180(3-4): 308-314.
- Karunakaran, C. & Dhanalakshmi, R. 2008. Photocatalytic performance of particulate semiconductors under natural sunshine - Oxidation of carboxylic acids. *Solar Energy Materials and Solar Cells* 92(5): 588-593.
- Khodja, A.A., Sehili, T., Pilichowski, J. & Boule, P. 2001. Photocatalytic degradation of 2-phenylphenol on TiO<sub>2</sub> and ZnO in aqueous suspensions. *Journal of Photochemistry and Photobiology A: Chemistry* 141(2-3): 231-239.
- Konstantinou, I.K. & Albanis, T.A. 2004. TiO<sub>2</sub>-assisted photocatalytic degradation of azo dyes in aqueous solution: Kinetic and mechanistic investigations: A review. *Applied Catalysis B: Environmental* 49(1): 1-14.
- Li, C., Chen, R., Zhang, X., Shu, S., Xiong, J., Zheng, Y. & Dong, W. 2011. Electrospinning of CeO<sub>2</sub>-ZnO composite nanofibers and their photocatalytic property. *Materials Letters* 65(9): 1327-1330.

- Lin, C.F., Wu, C.H. & Onn, Z.N. 2008. Degradation of 4-chlorophenol in TiO<sub>2</sub>, WO<sub>3</sub>, SnO<sub>2</sub>, TiO<sub>2</sub>/WO<sub>3</sub> and TiO<sub>2</sub>/SnO<sub>2</sub> systems. *Journal of Hazardous Materials* 154(1-3): 1033-1039.
- Liu, Z., Deng, J. & Li, F. 2008. Fabrication and photocatalysis of CuO/ZnO nano-composites via a new method. *Materials Science and Engineering B* 150(2): 99-104.
- Lizama, C., Freer, J., Baeza, J. & Mansilla, H.D. 2002. Optimized photodegradation of Reactive Blue 19 on TiO<sub>2</sub> and ZnO suspensions. *Catalysis Today* 76(2-4): 235-246.
- Nayak, J., Sahu, S.N., Kasuya, J. & Nozaki, S. 2008. CdS-ZnO composite nanorods: Synthesis, characterization and application for photocatalytic degradation of 3,4-dihydroxy benzoic acid. *Applied Surface Science* 254(22): 7215-7218.
- Pera-Titus, M., García-Molina, V., Baños, M.A., Giménez, J. & Esplugas, S. 2004. Degradation of chlorophenols by means of advanced oxidation processes: A general review. *Applied Catalysis B: Environmental* 47(4): 219-256.
- Pourata, R., Khataee, A.R., Aber, S. & Daneshvar, N. 2009. Removal of the herbicide Bentazon from contaminated water in the presence of synthesized nanocrystalline TiO<sub>2</sub> powders under irradiation of UV-C light. *Desalination* 249(1): 301-307.
- Rao, A.N., Sivasankar, B. & Sadasivam, V. 2009. Kinetic study on the photocatalytic degradation of salicylic acid using ZnO catalyst. *Journal of Hazardous Materials* 166(2-3): 1357-1361.
- Saien, J. & Khezrianjoo, S. 2008. Degradation of the fungicide carbendazim in aqueous solutions with UV/TiO<sub>2</sub> process: Optimization, kinetics and toxicity studies. *Journal of Hazardous Materials* 157(2-3): 269-276.
- Sobana, N. & Swaminathan, M. 2007. The effect of operational parameters on the photocatalytic degradation of Acid Red 18 by ZnO. *Separation and Purification Technology* 56(1): 101-107.
- Uddin, M.M., Hasnat, M.A., Samed, A.J.F. & Majumdar, R.K. 2007. Influence of TiO<sub>2</sub> and ZnO photocatalysts on adsorption and degradation behaviour of erythrosine. *Dyes and Pigments* 75(1): 207-212.
- Vaezi, M.R. 2008. Two-step solochemical synthesis of ZnO/TiO<sub>2</sub> nano-composite materials. *Journal of Materials Processing Technology* 205(1-3): 332-337.
- Wang, H., Xie, C., Zhang, W., Cai, S., Yang, Z. & Gui, Y. 2007. Comparison of dye degradation efficiency using ZnO powders with various size scales. *Journal of Hazardous Materials* 141(3): 645-652.
- Wu, P., Du, N., Zhang, H., Jin, L. & Yang, D. 2010. Functionalization of ZnO nanorods with  $\gamma$ -Fe<sub>2</sub>O<sub>3</sub> nanoparticles: Layer-by-layer synthesis, optical and magnetic properties. *Materials Chemistry and Physics* 124(2-3): 908-911.
- Xie, J., Li, Y., Zhao, W., Bian, L. & Wei, Y. 2011. Simple fabrication and photocatalytic activity of ZnO particles with different morphologies. *Powder Technology* 207(1-3): 140-144.

Lee Kian Mun

Department of Chemistry, Faculty of Science  
Universiti Putra Malaysia  
43400 Serdang, Selangor  
Malaysia

Abdul Halim Abdullah\*, Mohd Zobir Hussein  
& Zulkarnain Zainal  
Advanced Materials and Nanotechnology Laboratory  
Institute of Advanced Technology, Universiti Putra Malaysia  
43400 UPM Serdang, Selangor  
Malaysia

\*Corresponding author; email: halim@upm.edu.my

Received: 17 April 2013

Accepted: 12 July 2013